Identification and functional characterization of nonmammalian Toll-like receptor 20

Pietretti, D.; Scheer, M.; Fink, I.R.; Taverne, N.; Savelkoul, H.F.J.; Spaink, H.P.; ... ; Wiegertjes, G.F.

Immunogenetics (2014) 66:123–141
DOI 10.1007/s00251-013-0751-4

ORIGINAL PAPER

Identification and functional characterization of nonmammalian Toll-like receptor 20

Danilo Pietretti · Marleen Scheer · Inge R. Fink · Nico Taverne · Huub F. J. Savelkoul · Herman P. Spaink · Maria Forlenza · Geert F. Wiegertjes

Received: 10 October 2013 / Accepted: 26 November 2013 / Published online: 11 December 2013

Abstract Like other vertebrate Toll-like receptors (TLRs), the TLRs of teleost fish can be subdivided into six major families, each of which recognize a general class of molecular patterns. However, there also are a number of Tlrs with unknown function, the presence of which seems unique to the bony fish, among which is Tlr20. We identified full-length complementary DNA (cDNA) sequences for *tlr20* of zebrafish and common carp, two closely related fish species. Zebrafish have six copies of *tlr20*, whereas carp express only a single copy. Both zebrafish Tlr20 (at least Tlr20a–d) and carp Tlr20 have 26 leucine-rich repeats (LRRs). Three-dimensional modeling indicates a best fit to the crystal structure of TLR8. Phylogenetic analyses place Tlr20 in the TLR11 family closest to Tlr11 and Tlr12, which sense ligands from protozoan parasites in the mouse. Conservation of genes on zebrafish chromosome 9, which carries *tlr20*, with genes on mouse chromosome 14, which carries *tlr11*, indicates Tlr11 could be a possible ortholog of Tlr20. Confocal microscopy suggests a subcellular localization of Tlr20 at the endoplasmatic reticulum. Although in vitro reporter assays could not identify a ligand unique to Tlr20, in vivo infection experiments indicate a role for Tlr20 in the immune response of carp to protozoan parasites (*Trypanoplasma borreli*). Carp *tlr20* is mainly expressed in peripheral blood leukocytes (PBL) with B lymphocytes, in particular, expressing relatively high levels of *Tlr20*. In vitro stimulation of PBL with *T. borreli* induces an upregulation of *tlr20*, supportive of a role for Tlr20 in the immune response to protozoan parasites.

Keywords Toll-like receptors · Tlr20 · Tlr11 · Teleost · Evolution · Innate immunity

D. Pietretti · M. Scheer · I. R. Fink · H. F. J. Savelkoul · M. Forlenza · G. F. Wiegertjes (✉)
Cell Biology and Immunology Group, Wageningen Institute of Animal Sciences, Wageningen University, PO Box 338, 6700 AH Wageningen, The Netherlands
e-mail: geert.wiegertjes@wur.nl

N. Taverne
Host-Microbe Interactomics Group, Wageningen Institute of Animal Sciences, Wageningen University, PO Box 338, 6700 AH Wageningen, The Netherlands

H. P. Spaink
Institute of Biology, Leiden University, Einsteinweg 55, 2333 CC Leiden, The Netherlands

Introduction

Toll-Like receptors (TLRs) play an important role in innate immune mechanisms that form the first line of defense against invading pathogens. TLRs are a group of pattern-recognition receptors (PRRs) recognizing conserved molecular motifs also named pathogen-associated molecular patterns (PAMPs). Recognition of PAMPs by TLRs not only activates the innate immune system but also activates pathways important for acquired immunity (Medzhitov et al. 1997). TLRs typically are type I transmembrane proteins composed of three different domains; an extracellular domain (ECD) characterized by a horseshoe shape containing a large number of LRRs of 20–30 amino acids important for the recognition of PAMPs, a transmembrane domain and an intracellular Toll/interleukin-1 receptor (TIR) domain that initiates intracellular signaling (Akira et al. 2006).

Most vertebrate genomes have at least one gene representing each of six major TLR families (TLR1, TLR3, TLR4, TLR5, TLR7, and TLR11), each recognizing a general class of molecular patterns (Pietretti et al. 2013; Roach et al. 2005). The ECD of TLRs, important for ligand recognition, can consist of 16–28 LRRs; often, the total number of LRRs can be linked with one of the six major families (Matsushima et al. 2007). Although most vertebrate genomes have TLR genes in each of the six major

families, not all vertebrates express the exact same repertoire. For example, the human genome contains 10 functional TLRs, whereas the mouse genome contains 12 Tlrs, with *tlr10* being a pseudogene and *tlr11*, *tlr12*, and *tlr13* being mouse-specific (Ariffin and Sweet 2013). Murine Tlr11 and Tlr12 sense profillin from *Toxoplasma gondii* (Koblansky et al. 2013; Yarovinsky et al. 2005), whereas Tlr13 was recently described as a sensor of bacterial 23S rRNA (Oldenburg et al. 2012). The latter Tlrs (Tlr11, Tlr12, and Tlr13) are the best-described members of the large TLR11 family, which also includes a number of nonmammalian Tlrs, among which Tlr20 the subject of the present study.

To date, a total number of 26 Tlrs have been identified across different vertebrate species based on teleost, amphibian, and avian genomes (Brownlie and Allan 2011; Ishii et al. 2007; Quiniou et al. 2013; Rebl et al. 2010; Roach et al. 2005). At present, the TLR11 family not only contains Tlr11–13 from the mouse but also nonmammalian Tlr15, Tlr16, Tlr17, Tlr19, Tlr20, Tlr21, Tlr22, Tlr23, and Tlr24 (Palti 2011; Quiniou et al. 2013). Of these TLR11 family members, full sequences have been reported for Tlr15 and Tlr16 in chicken (Keestra et al. 2007; Yilmaz et al. 2005), Tlr19 and Tlr20 in zebrafish and channel catfish (Meijer et al. 2004; Quiniou et al. 2013), Tlr21 in several fish species and in chicken (Brownlie et al. 2009; Meijer et al. 2004; Oshiumi et al. 2003; Quiniou et al. 2013), Tlr22 in several fish species (Meijer et al. 2004; Oshiumi et al. 2003; Quiniou et al. 2013; Roach et al. 2005; Sundaram et al. 2012), and Tlr23 in pufferfish and Atlantic cod (Roach et al. 2005; Sundaram et al. 2012). Ligand recognition and exact function of the nonmammalian TLR11 family members remain undefined, with the one exception of Tlr22 that has been reported to sense long-sized double-stranded RNA on the cell surface (Matsuo et al. 2008). With regard to Tlr20, already in one of the first studies on teleost Tlrs, multiple but partial Tlr20 sequences (*tlr20a–f*) were identified in the zebrafish genome (Meijer et al. 2004), followed by partial sequences for Tlr20 in rainbow trout (Palti et al. 2006) and channel catfish (Baoprasertkul et al. 2007). Only very recently, a full-length *tlr20* sequence was described for channel catfish (Quiniou et al. 2013). Nevertheless, functional studies on teleost Tlr20 have not been reported.

We characterize for the first time in detail Tlr20 of zebrafish and common carp, two cyprinid fish species that are closely related (Henkel et al. 2012). Teleost Tlr20 has the conserved features of mammalian TLRs with an ECD containing 24–26 LRRs, a conserved intracellular TIR domain and both an N- and C-terminal LRR (LRRNT and LRRCT). Leucine-rich repeats are often flanked by N- and C-terminal cysteine-rich domains (LRRNT and LRRCT) (Park et al. 2008). Teleost Tlr20s cluster with mouse Tlr11 and Tlr12, both members of the TLR11 family. We used a three-dimensional modeling approach to find a best fit for teleost Tlr20 to known TLR crystal structures and used a synteny approach to examine the genomic conservation of genes adjacent to zebrafish Tlr20. Confocal microscopy was used to study subcellular localization of Tlr20 in human and fish cell lines transfected with carp Tlr20. In vitro reporter assays based on nuclear factor kappa B (NF-κB) activation following stimulation of a human cell line overexpressing carp Tlr20 were used to identify putative ligands of Tlr20. In vivo infection experiments allowed for an investigation of *tlr20* gene expression induced by protozoan parasites (*Trypanoplasma borreli*) of carp. Screening of a cDNA library of carp tissues and leukocyte subtypes indicated that carp *tlr20* is highly expressed in peripheral blood leukocytes (PBL), in particular B lymphocytes, relative to other leukocyte cell types. In vitro stimulation of carp PBL and re-stimulation of PBL from fish that survived a *T. borreli* infection with parasite lysate, induced an upregulation of *tlr20*, supportive of a role for Tlr20 in the immune response of carp to protozoan parasites.

Materials and methods

Animals

European common carp (*Cyprinus carpio carpio*) were reared in the central fish facility of Wageningen University at 23± 2 °C in recirculating UV-treated water and fed pelleted dry food (Sniff, Soest, Germany) daily. R3xR8 heterozygous carp (9–11 months old) were the offspring of a cross between fish of Hungarian (R8 strain) and of Polish (R3 strain) origin (Irnazarow 1995). All studies on carp were performed with approval from the animal experimental committee of Wageningen University. Zebrafish (*Danio rerio*) were reared in the central fish facility of Leiden University at 28±2 °C in compliance with the local animal welfare regulations and maintained according to standard protocols (zfin.org) in recirculating UV-treated water and fed flakes (Tetra, Melle, Germany) daily.

Isolation of immune organs and purification of leukocyte subtypes

Total RNA was isolated from different carp organs (Forlenza et al. 2008b) and from different leukocyte subtypes purified by magnetic cell sorting using specific antibodies as described before for head kidney-derived macrophages (Joerink et al. 2006), thrombocytes (Rombout et al. 1996), thymocytes (Stolte et al. 2008), granulocytes (Forlenza et al. 2008b), and B cells (Koumans-van Diepen et al. 1995; Secombes et al. 1983).

PBLs were obtained from carp blood first centrifuged for 5 min at 100×*g* and then for 10 min at 600×*g* to obtain the buffy coat. The buffy coat was layered on 3 ml Ficoll-Paque™ Plus (Amersham Biosciences) and centrifuged at

800×*g* for 25 min. PBL were collected, washed three times in culture medium (RPMI 1640 adjusted to 270 mOsmol kg^{-1}) (Cambrex), and counted. For stimulation assays, PBL were seeded at a concentration of 0.5×10^6 cells/well in 96-well culture plates and stimulated with *T. borreli* lysate (equivalent of 1:2 parasites/cells) or with culture medium alone as negative control for 3, 6, and 24 h. After incubation, cells were collected for RNA isolation.

RNA isolation and cDNA synthesis

RNA was isolated using Trizol® (Invitrogen, Breda, The Netherlands) according to the manufacturer's protocol and stored a −80 °C until use. RNA concentration was measured spectophotometrically (GeneQuant, Pharmacia Biotech) at OD_{260nm}, and the purity determined as the OD_{260nm}/OD_{280nm} ratio with expected values between 1.8 and 2.0. The integrity of RNA was determined by gel electrophoresis on 1 % agarose gel containing 0.1 % of SYBR® Safe DNA Gel Stain (Invitrogen™).

cDNA synthesis was performed with 1 μg total RNA using DNase I amplification grade (Invitrogen) according to the manufacturer's instructions. Synthesis of cDNA was performed with Invitrogen's SuperScript™ III First-Strand Synthesis Systems for RT-PCR, according to the manufacturer's instructions. A nonreverse transcriptase control was included for each sample. Before use as template in real time-quantitative PCR (RT-qPCR) analysis, the cDNA was further diluted 25–50 times in nuclease-free water.

Molecular cloning of zebrafish *tlr20*

The initial in silico prediction of six zebrafish *tlr20* genes in the genome of zebrafish (Meijer et al. 2004) was used to detect *tlr20* in the most recent zebrafish genome assembly Zv9 (GCA_000002035.2) using Genomics Workbench version 4.9 (CLC Bio, Aarhus, Denmark). The putative coding regions within the genomic DNA were identified using FGENESH, and the predicted amino acid sequences were confirmed using these sequences as template in BLAST (Altschul et al. 1990) and FAST (Pearson and Lipman 1988).

Molecular cloning of carp *tlr20*

Carp *tlr20* was first identified in the draft genome of common carp (Bioproject PRJNA73579) (Henkel et al. 2012) using zebrafish *tlr20a* (accession number AAI63786) as reference sequence for the BLAST search. We identified one contig within the carp genome (contig 28896) with a region coding for a single Tlr20 sequence. Gene-specific primers to amplify the full-length coding sequence (CDS) were designed using the Primer3 program (http://bioinfo.ut.ee/primer3-0.4.0/primer3/). As template we used cDNA synthesized using a LongRange 2Step RT-PCR kit (Qiagen) from RNA collected from head kidney tissue taken from carp 3 weeks after infection with the parasite *Trypanosoma carassii* (Joerink et al. 2006). A first PCR to obtain the full-length carp *tlr20* CDS was performed using the Expand High Fidelity Plus PCR System (Roche) followed by a second PCR using tlr20Fw- and tlr20Rv-specific primers (see Table 1). The product was cloned in JM109 competent *Escherichia coli* cells using the pGEM-TEasy kit (Promega), and both strands of eight positive clones were sequenced using the ABI Prism-Bigdye Terminator Cycle Sequencing Ready Reaction kit, and analyzed using an ABI 3730 sequencer. Nucleotide sequence data were analysed for identity to other sequences using the GenBank database (Benson et al. 1999).

Bioinformatics and synteny analysis

Nucleotide sequences of *tlr20* were translated using the ExPASy *Translate* tool (http://us.expasy.org/tolls/dna.html) (Gasteiger et al. 2003) and aligned with Multiple Sequence Alignment by ClustalW (http://www.genome.jp/tools/clustalw/). The predicted amino acid sequences were examined for the presence of a signal peptide using the SignalP (http://www.cbs.dtu.dk/services/SignalP-2.0/), Predisi (http://www.predisi.de/) (Nielsen et al. 1997), and TMHMM2.0 programs (http://www.cbs.dtu.dk/services/TMHMM-2.0/). Identification of protein domains was done with SMART (Letunic et al. 2012) (http://smart.embl-heidelberg.de/) and LRRfinder (http://www.lrrfinder.com/). Individual LRRs were identified manually according to prior definitions (Bell et al. 2003; Matsushima et al. 2007) and three-dimensional modeling. A phylogenetic tree based on the TIR intracellular domains was constructed using the neighbor-joining method (Saitou and Nei 1987) using MEGA5 software (Tamura et al. 2011). Evolutionary distances were computed using the Poisson correction method (Zuckerkandl and Pauling 1965), all positions containing gaps and missing data were eliminated from the dataset (complete deletion option). Phylogenetic analyses were done with 10,000 bootstrap replicates. Genome synteny of the loci harboring *tlr20* was examined by comparing the genomes of mouse (GCA_000001635.3), carp (PRJNA73579), and zebrafish (GCA_000002035.2) retrieved from the Ensemble Genome Browser (Flicek et al. 2012) (http://www.ensembl.org/index.html).

Three-dimensional modeling

Structural models were obtained using the amino acid sequence alignment of carp Tlr20 and human TLR8, and the available dimer crystal structure of human TLR8 (PDB-id: 3w3g) as template using the Modeller program (version 9.12) (Šali and Blundell 1993). The *N*-acetylglucosamine (NAG), β-D-mannose, and water molecules present in the crystal

Table 1 Primers used

Primer	Sequence (5′–3′)	Used
tlr20Fw	ATTGAAGATGGTGCCTCTGTTC	Cloning
tlr20Rv	TAGAGAAATGAAGTTTAGTTGG	Cloning
q40SFw	CCGTGGGTGACATCGTTACA	RT-qPCR
q40SRv	TCAGGACATTGAACCTCACTGTCT	RT-qPCR
qtlr20Fw	ATTATGTGACCGTTGAGGGCTGC	RT-qPCR
qtlr20Rv	TCCAGATTGACGACCGATCTTAC	RT-qPCR
cyca-tlr20-HA-Fw1	TTGTTCTTGGCTTGCT**TACCCATACGATGTTCCAGATTACGCT**GATAAATGCCTTTTCTACAGTGATG	HA-Tlr20-GFP
cyca-HA-tlr20-*Bam*HI-Fw2	TGAGGGATCCAACATGGTGCCTCTGTTCTCGCTCTTCATACTGTTTCTGAAGACTTCATGCATTTGTTCTTGGCTTGCT**TACCCATACGATGTTCCAGATTACGCT**GATAAATGCCTTTTCTACAGTGATG	HA-Tlr20-GFP
cyca-tlr20-*Bam*HI-Fw3	TGAGGGATCCAACATGGTGCCTCTGTTCTCGCTCT	HA-Tlr20-GFP
cyca-tlr20-*Xho*I-Rv1	GGAACTATACAATATAGAGAAATGACTCGAGGTTGGT	HA-Tlr20-GFP

Bold sequence indicates the HA tag (**TACCCATACGATGTTCCAGATTACGCT**); underlined sequence indicates the *Bam*HI restriction site (GGATCC); double underlined sequence indicates the *Xho*I restriction site (CTCGAG)

structure were included in the modeling procedure. Thirty comparative models were generated, after which the model with lowest corresponding DOPE score (Eswar et al. 2006) was selected for image generation with Pymol, an OpenGL based molecular visualization system.

HA-Tlr20-GFP expression plasmid

The PCR product amplifying the complete carp *tlr20* CDS was used as template for a PCR using as primers cyca-tlr20-HA-Fw1 in combination with cyca-tlr20-*Xho*I-Rv1 (primers listed in Table 1) followed by a second PCR using cyca-HA-tlr20-*Bam*HI-Fw2 in combination with cyca-tlr20-*Xho*I-Rv1. The PCR products were purified and used as template for a final PCR using cyca-tlr20-*Bam*HI-Fw3 and cyca-tlr20-*Xho*I-Rv1. Primers were designed to add a *Bam*HI site at the 5′ end, upstream of the signal peptide and the hemagglutinin (HA)-tag sequence, and an *Xho*I site at the 3′ end, excluding the *tlr20* stop codon. Subsequently, this product was ligated into the *Bam*HI and *Xho*I sites of a pcDNA3.1 plasmid (Promega) in frame with the sequence of the green fluorescent protein (GFP) that was already inserted in the vector, to obtain the HA-Tlr20-GFP fusion product.

Subcellular localization of Tlr20

Computational prediction of the subcellular localization of zebrafish and carp Tlr20 was performed with the TargetP program (http://www.cbs.dtu.dk/services/TargetP/) (Nielsen et al. 1997). Experimental determination of the subcellular localization was performed using the carp HA-Tlr20-GFP construct. To this end, a human cell line (human embryonic kidney cells, HEK 293) and three fish cell lines: epithelioma papulosum cyprini (EPC) (Fijan et al. 1983), carp leukocyte culture (CLC) (Faisal and Ahne 1990), and zebrafish embryonic fibroblast 4 (ZF4) (Driever and Rangini 1993) were used. Both HEK 293 and ZF4 cells were cultured in Dulbecco's Modified Eagle Medium F12 (Gibco®) medium supplemented with 10 % fetal bovine serum (FBS), 1 % L-glutamin, and 1 % streptomycin/penicillin at 37 °C (HEK) or at 27 °C (ZF4) with 5 % CO_2. Both EPC and CLC cells were cultured in RPMI 1640 (Cambrex) supplemented with 10 % FBS, 1 % L-glutamin and 1 % streptomycin/penicillin at 27 °C with 5 % CO_2.

HEK 293, EPC, and CLC cells were seeded in six-well plates [0.5×10^6 cells/well (HEK 293) and 1×10^6 cells/well (EPC and CLC)] 24 h prior to transfection. Cells were transfected with 2 μg of carp HA-Tlr20-GFP plasmid using jetPRIME (Polyplus; HEK 293) or FuGENE 6 (Roche Molecular Biochemicals; EPC or CLC) all according to the manufacturer's instructions.

ZF4 cells were seeded 24 h prior to transfection on glass bottom culture dishes (P35G-0-14-C, MatTek corporation Ashland) at 2×10^4 cells/dish in a volume of 500 μl medium. ZF4 cells were (co)-transfected using jetPRIME with 0.3 μg HA-Tlr20-GFP plasmid and 0.2 μg red fluorescent protein Vector-endoplasmic reticulum (ER) plasmid (RFP-KDEL, catalog number 558725 BD Pharmingen™), the latter containing a KDEL sequence that specifically targets the ER. For ER localization ZF4 cells were used because they are particularly suitable for live imaging of cell compartments because they adhere by stretching.

Four hours post-transfection, medium was replaced with 3 ml complete medium. Subcellular localization was determined 2–3 days after transfection with the help of a Zeiss LSM-510 laser scanning microscope. Green fluorescent signal (rhodamine or green-fluorescent protein) was excited with a 488-nm argon laser and detected using a band-pass filter (505–530 nm). Red-fluorescent signal (propidium iodide)

was excited with a 543-nm helium–neon laser and detected using a long-pass filter (560 nm).

To distinguish between intra- and extracellular localization of carp HA-Tlr20-GFP, cells (HEK 293, EPC, and CLC) were harvested 72 h posttransfection and fixed with 4 % paraformaldehyde for 15 min at room temperature (RT), followed by a washing step with phosphate-buffered saline (PBS) containing 1 % (*w*/*v*) bovine serum albumin (PBS-BSA). Cells were incubated with mouse anti-HA antibody (Cell Signaling Technology ™) for 1 h at RT and washed with PBS-BSA followed by incubation with donkey antimouse-Cy3 antibody (Merck Millipore) for 1 h at RT in the dark and followed by a washing step. For intracellular localization, prior to incubation with the anti-HA antibody, cells were permeabilized by resuspension in 100 μl of 0.05 % (*v*/*v*) Triton X-100 in PBS-BSA and incubation for 20 min at RT followed by a washing step with PBS-BSA. Nuclei were stained with VECTAS HIELD® Mounting Media containing propidium iodide (Vector Laboratories) after overnight incubation.

In vitro ligand studies

HEK 293 cells were transfected with 3.5 μg of pNiFty-Luc, a plasmid encoding for the luciferase reporter gene under the control of the NF-κB-inducible ELAM-1 composite promoter (InvivoGen). Stably transfected cells (HEK-NFκB-Luc) were selected using 250 μg/ml Zeocin (Life technologies™). For transient transfection of the HA-Tlr20-GFP vector, stably transfected HEK-NFκB-Luc cells were first plated at 5×10^4 cells/well in a 96-well plate and incubated for 24 h, followed by transfection with 0.125 μg of carp HA-Tlr20-GFP vector. Alternatively, cells were transfected with the same amount of a pcDNA3-GFP plasmid as negative control, or with pcDNA3-TLR2-YFP (Addgene plasmid 13016 encoding for human TLR2) as positive control and incubated for 72 h. After this incubation period, cells were stimulated with different ligands for 5 h, medium was replaced with Bright glow (Promega), the suspension transferred to a white 96 well plate with opaque bottom (Corning®, catalogue number 3300) and luminescence measured (Filtermax 5, Molecular Devices).

Cells were stimulated with recombinant human tumor necrosis factor alpha or with one of the following TLR ligands (all InvivoGen): synthetic diacylated lipopeptide Pam_2CSK_4 (tlrl-pm2s), ultrapure LPS from *E. coli* O111:B4 (tlrl-eblps), ultrapure lipopolysaccharide from *Porphyromonas gingivalis* (tlrl-pgLPS), purified lipoteichoic acid from *Staphylococcus aureus* (tlrl-psLTA), ultrapure endotoxin-free single-stranded DNA from *E. coli* (tlrl-ssec), CpG ODNs 1668 (tlrl-1668), polyinosinic-polycytidylic acid (tlrl-pic), flagellin from *S. typhimurium* (tlrl-stfla), and 23S rRNA (ORN Sa19) from *S. aureus* (tlrl-orn19). Parasite lysates of *T. borreli* were made by washing column-purified parasites (1×10^8 parasites/ml) (Ruszczyk et al. 2008) in carp RPMI, and lysing by sonication. Lysates were stored at −80 °C until use. Profillin from *T. gondii* (ALX-522-093-C010) was purchased from Enzo® Life Sciences.

Real-time quantitative polymerase chain reaction

To investigate gene expression of *tlr20*, RT-qPCR was performed using ABsolute QPCR SYBR Green Mix (no Rox) (Thermoscientific) with a Rotor-Gene™ 6000 (Corbett Reasearch) as previously described (Forlenza et al. 2012). Primers used for RT-qPCR were designed to amplify the S11 protein of the 40S subunit (40S) as a reference gene or designed to amplify carp tlr20 (see Table 1) using OligoAnalyser 3.1 IDT (Integrated DNA Technologies) (http://eu.idtdna.com/analyzer/applications/oligoanalyzer/default.aspx). To 7 μl SYBR Green master mix containing forward and reverse primers (300 nM each), 5 μl of 50 times-diluted cDNA, was added. The following cycling conditions were used: one holding step of 15 min at 95 °C; followed by 40 cycles of 15 s at 95 °C for denaturation, 20 s at 60 °C for annealing and 20 s at 72 °C for elongation, followed by a final holding step of 1 min at 60 °C. A melting curve was then created with continuous fluorescence acquisition starting at 60 °C with a rate of 0.5 °C/5 s up to 90 °C to determine the amplification specificity. In all cases, amplification was specific and no amplification was observed in negative control samples (nontemplate control and nonreverse transcriptase control). Fluorescence data from RT-qPCR experiments were analysed using Rotor-Gene software version 1.7 (built 87) and exported to Microsoft Excel. Relative expression ratios were obtained using the Pfaffl method (Pfaffl 2001) using average efficiencies per run, per gene. Gene expression of the house keeping gene was highly constant as determined by the BestKeeper software (Pfaffl et al. 2004) and used to normalize the data. Each PCR product was checked at least once by sequencing.

In vivo infection with *Trypanoplasma borreli*

Infections with extracellular blood parasites *T. borreli* were performed as described previously (Forlenza et al. 2008b). Briefly, *T. borreli* was maintained by syringe passage through carp following intraperitoneal (i.p.) injections with 1×10^4 parasites per fish. Before infection with *T. borreli*, carp were anesthetized in 0.3 g/l tricaine methane sulfonate (Crescent Research Chemicals, Phoenix, USA) and i.p. injected with *T. borreli* or with PBS as noninfected control. At various time points after infection, fish were euthanized with an overdose of anesthetic.

Statistical analysis

Relative expression ratios (R) were calculated as described above. Transformed [LN(R)] values were used for statistical

analysis in GraphPad prism version 5. For all tests, homogeneity of variance was assessed using Levene's test. Significant differences ($P<0.05$) were determined by two-way ANOVA followed by Sidak test. In case of unequal variances between groups, a two-way ANOVA was performed followed by a Games–Howell test for the infection studies with parasites. For studies on constitutive gene expression levels, significance of differences was determined by one-way ANOVA as compared to values in organs or cell types with the lowest values.

Results

Identification of multiple zebrafish Toll-like receptor 20 genes

In a previous genome analysis of the Toll-like receptor families of zebrafish, the presence of six zebrafish *tlr20* genes was predicted in silico (Meijer et al. 2004). More detailed analysis of the latest zebrafish genome assembly Zv9 confirmed the presence of six *tlr20* genes. Zebrafish *tlr20b*, *tlr20a*, *tlr20c*, and *tlr20d* are located (in this order) adjacent to each other on one part of chromosome 9 (region: 28388211–28414876), whereas *tlr20f* and *tlr20e* are also located next to each other but on a different part of chromosome 9 (region: 31239519–31278948), distant from the other *tlr20 genes* (see also Fig. 4). However, the latter two copies (*tlr20f* and *tlr20e*) contain mutations in the reading frame that prevent gene expression, in one case leading to a premature stop codon. This supports the prediction that two of the six copies of zebrafish *tlr20* are pseudogenes. The full-length sequences (*tlr20b*, *tlr20a*, *tlr20c*, and *tlr20d*) have open reading frames ranging from 2,826 to 2,853 bp encoding for proteins of 942–951 aa (Fig. 1) with predicted molecular weights of 124.7–126.0 kDa. Leucine-rich repeats are flanked by N- and C-terminal cysteine-rich domains (LRRNT and LRRCT). The four full-length zebrafish Tlr20 molecules all have an N-terminal leucine-rich repeat (LRRNT) ($Cx_{14}Cx_8C$ or $Cx_{23}C$), a C-terminal LRR (LRRCT) ($CxC_{28}Cx_{18}C$) and 26 LRR, a transmembrane domain and Toll/IL-1R domain (TIR) (see also Tables 2 and 3). Zebrafish Tlr20 molecules (*tlr20a–d*) have a signal peptide of 19–25 aa indicating that they are targeted to the secretory pathway.

Identification of a single Toll-like receptor 20 (*tlr20*) in carp

A putative *tlr20* sequence was identified in the draft genome of common carp based on open reading frame prediction and BLAST alignment with zebrafish *tlr20a*. A single exon containing carp *tlr20* was predicted from contig 28896, and this sequence was used to clone the full-length carp *tlr20* cDNA (GenBank accession number KF482527). We obtained a complete cDNA sequence with open reading frame of 2,841 bp, encoding for a protein of 946 aa with a predicted molecular weight of 124.97 kDa. Carp Tlr20 is predicted to contain a signal peptide of 22 aa, an N- and a C-terminal leucine rich repeat (LRRNT, LRRCT) and 26 LRRs, a transmembrane domain and a TIR domain (see Fig. 1). Multiple sequence alignments of carp Tlr20 with the four full-length zebrafish Tlr20 and with channel catfish (*Ictalurus punctatus*) Tlr20-1 showed a high degree of conservation.

Tlr20 three-dimensional modeling and phylogeny

The three-dimensional structure of carp Tlr20 was modeled using as best fit the crystal structure of human TLR8 (PDB-id: 3w3g). Carp Tlr20 showed a good three-dimensional fit with the dimer structure of human TLR8, composed of two copies arranged in a symmetrical manner (Fig. 2). Mammalian TLR8 is known to contain 27 LRRs, a characteristic of the TLR7 family that includes TLR7, TLR8, and TLR9. Although Tlr20 has (only) 26 LRR, the human TLR8 model showed the best fit. TLRs from the TLR7 family have a 58–73-residue loop between LRR15 and LRR16 (Matsushima et al. 2007), whereas carp Tlr20 has a shorter, 13-residue loop between LRR15 and LRR16. The biological consequence, if any, of these slight differences is unknown.

Phylogenetic analysis was conducted based on the amino acid sequences of the TIR domain of known Tlrs from common carp, zebrafish and channel catfish in comparison with Tlrs from the mouse (Fig. 3). Phylogenetic analysis supported previous observations that fish have at least one gene representing each of six major TLR families (TLR1, TLR3, TLR4, TLR5, TLR7, and TLR11). The TLR11 family presently includes Tlr11, Tlr12, and Tlr13 (mouse) and Tlr19, Tlr20, Tlr21, Tlr22, and Tlr26 (nonmammalian Tlrs). Within the Tlr11 family, not only Tlr19 but also Tlr21 and Tlr22 branched off close to Tlr13 from the mouse. Tlr20 and Tlr26

Fig. 1 Multiple amino acid alignment of Tlr20 shows conservation of leucine-rich repeat (*LRR*), transmembrane (*TM*), and toll/interleukin-1 (*TIR*) domains. Multiple alignment of amino acid sequences from common carp (*Cyprinus carpio*) Tlr20 (KF482527), zebrafish (*Danio rerio*) Tlr20a (ENSDARG00000094411), Tlr20b (ENSDARG00000092668), Tlr20c (ENSDARG00000041164), Tlr20d (ENSDARG00000088701), and channel catfish (*Ictalurus punctatus*) Tlr20-1 (AEI59676). Alignment was performed using ClustalW v2.0. The putative signal peptide is *underlined*. Predicted leucine-rich repeat domains are highlighted in *gray* and *numbered LRR1–LRR26*. Conserved cysteine residues important for the LRRNT and LRRCT domains are indicated by *arrows* above the sequence alignment. The transmembrane region is *underlined*, whereas the TIR domain is highlighted in *black*. *Asterisks* indicate identities, *double dots* conserved substitutions, *single dots* semiconserved substitutions, and *dashes* gaps used to maximize the alignment. A predicted, but not yet confirmed Tlr20 (AGKD01003001) from the genome of Atlantic salmon (*Salmo salar*) and an incomplete Tlr20-2 (AEI59677) from channel catfish (Quiniou et al. 2013) were not included in the alignment

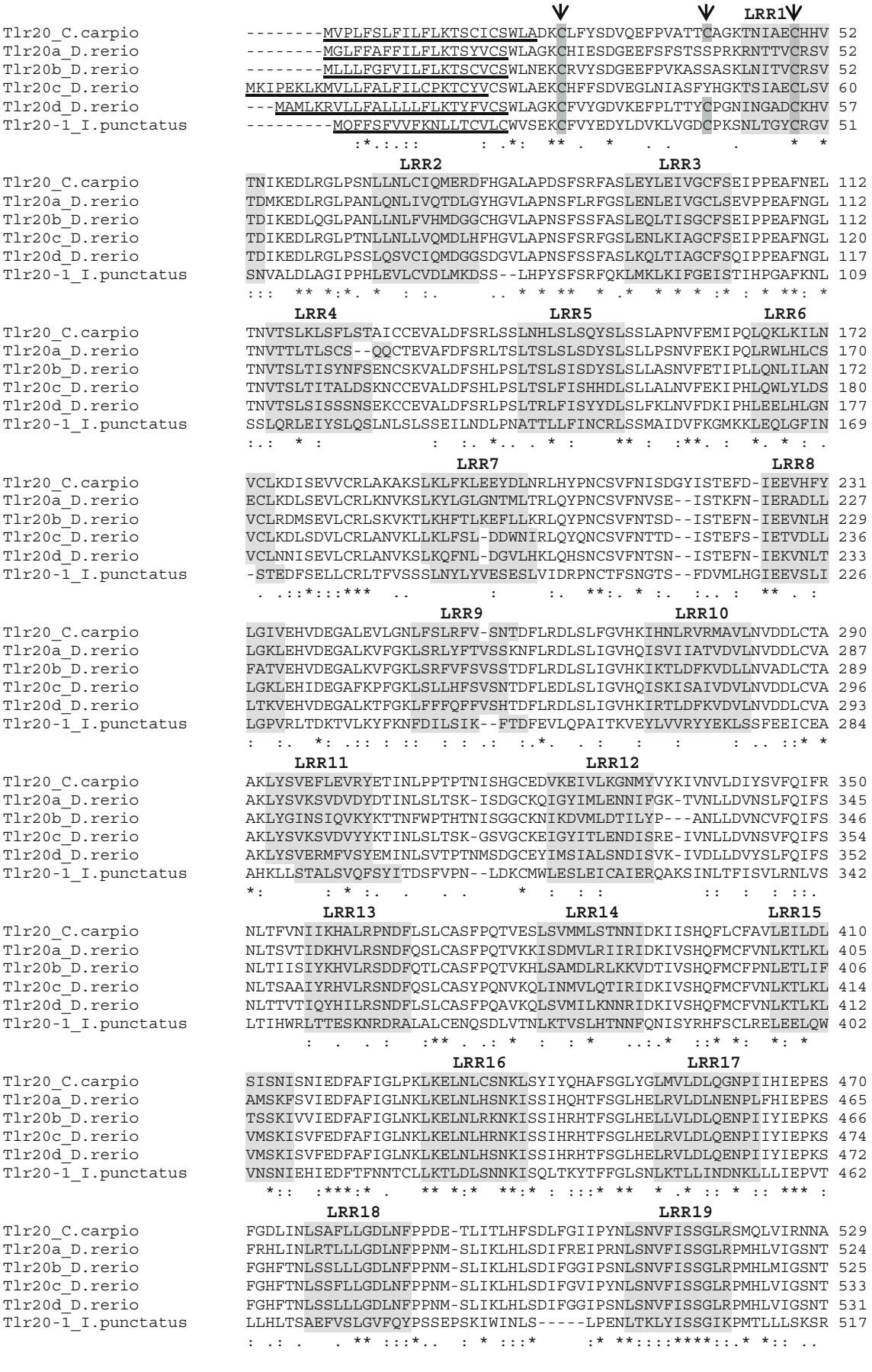
LRR1
LRR2
LRR3
LRR4
LRR5
LRR6
LRR7
LRR8
LRR9
LRR10
LRR11
LRR12
LRR13
LRR14
LRR15
LRR16
LRR17
LRR18
LRR19
Tlr20_C.carpio
Tlr20a_D.rerio
Tlr20b_D.rerio
Tlr20c_D.rerio
Tlr20d_D.rerio
Tlr20-1_I.punctatus

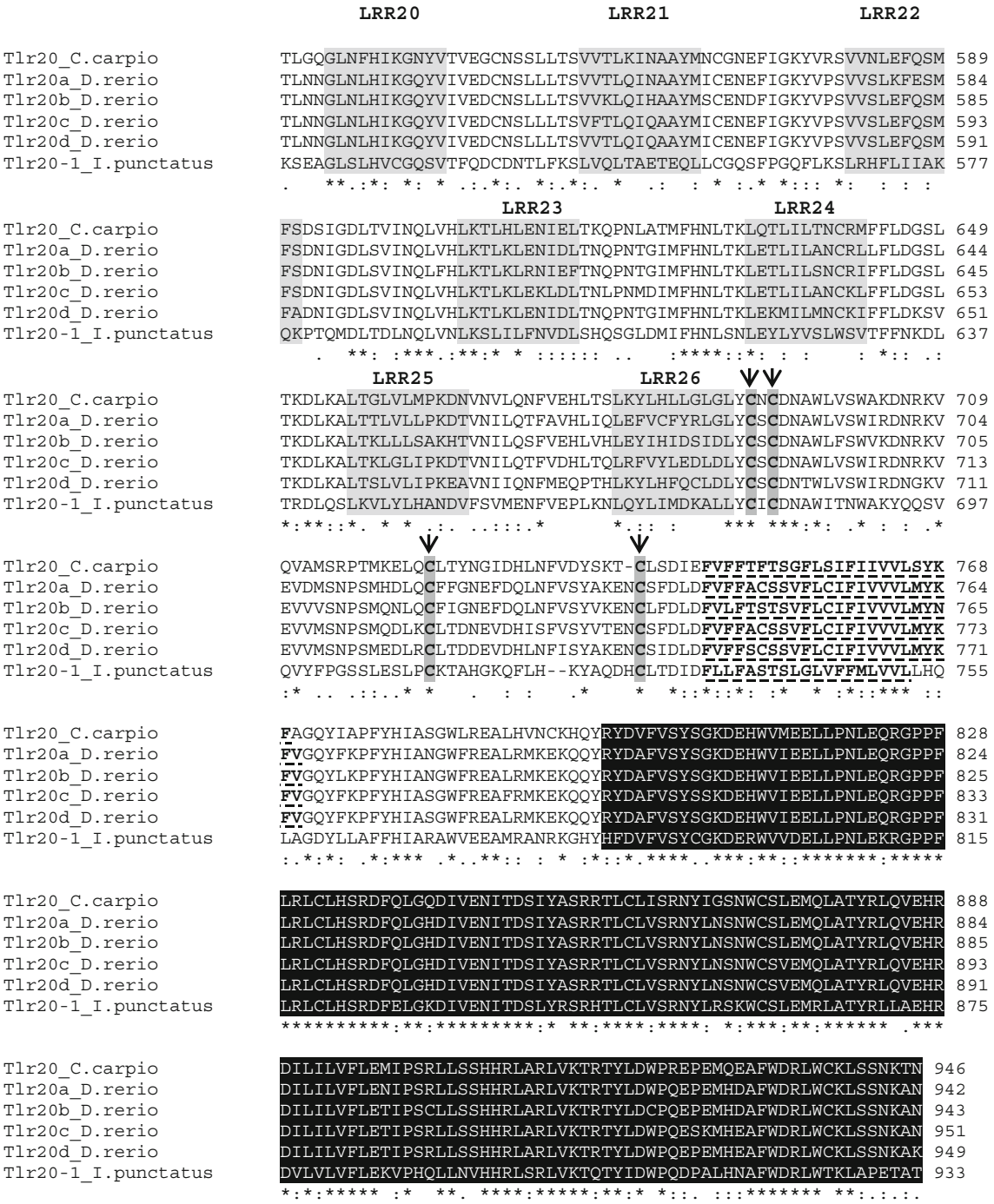

Fig. 1 (continued)

(channel catfish) branched off close to Tlr11 and Tlr12 (mouse), suggesting that teleost Tlr20 share a common ancestor with Tlr11/Tlr12.

Sequence and synteny analysis of Tlr20

In general, similarity was high comparing carp and zebrafish sequences, especially between TIR domains (Table 2), but lower comparing carp or zebrafish with sequences of channel catfish. Sequence analysis confirmed conservation of structural features of TLR20s including $n=26$ LRRs, presence of LRRNT and LRRCT, transmembrane domain, and, in particular, the intracellular TIR domain (aa identity>60 %) (Table 2).

The extracellular domain of TLRs, important for the recognition of PAMPs, can consist of 16–28 LRRs. The TLR11 family members have 20–28 LRR (Matsushima et al. 2007). LRRs are sometimes difficult to predict using programs such

Table 2 Comparison of amino acid identity of extracellular and TIR domains of Tlr20

Name		*C. carpio*	*D. rerio*				*I. punctatus*	*M. musculus*		
		Tlr20	Tlr20a	Tlr20b	Tlr20c	Tlr20d	Tlr20-1	Tlr11	Tlr12	Tlr13
C. carpio	Tlr20		63.7	63.9	63.9	64.7	38.4	14.9	16.3	14.3
D. rerio	Tlr20a	*86.0*		72.2	76.9	71.8	34.4	18.3	14.9	16.6
	Tlr20b	*84.9*	*95.5*		71.9	71.6	37.1	16.5	17.5	13.9
	Tlr20c	*84.5*	*96*	*92.5*		74.4	34.4	15.3	16.3	14.0
	Tlr20d	*86.0*	*97*	*64.0*	*97.0*		36.4	17.4	14.2	17.1
I. punctatus	Tlr20-1	*64.1*	*65.7*	*66.7*	*64.1*	*59.1*		21.2	19.2	19.9
M. musculus	Tlr11	*32.5*	*33.5*	*33.7*	*33.0*	*21.1*	*35.3*		33.0	17.0
	Tlr12	*44.9*	*45.6*	*44.9*	*44.2*	*29.2*	*47.6*	*51.0*		18.7
	Tlr13	*44.0*	*45.3*	*44.6*	*44.6*	*26.4*	*42.8*	*32.7*	*40.1*	

Numbers (top right triangle) indicate percentage identity of the extracellular domains (ECD). Italicized numbers (lower left triangle) indicate percentage identity of the intracellular TIR domain

as SMART or LRR-finder; therefore, we predicted LRRs manually and by three-dimensional modeling of carp Tlr20. The number of LRRs for teleost Tlr20 and mouse Tlr11-13, including presence of LRRNT and LRRCT, is listed in Table 3. All Tlr20 molecules from carp, zebrafish and channel catfish, except the channel catfish Tlr4-2, have an identical number of 26 LRRs. In mouse, Tlr11, Tlr12, and Tlr13 have 25, 24, or 27 LRRs, respectively. The $Cx_{14}Cx_8C$ LRRNT motif is shared among teleost Tlr20, with the exceptions of zebrafish Tlr20b and Tlr20c ($Cx_{23}C$). The LRRCT motif of the Tlr20 molecules is comparable among the different teleosts ($CxCx_{28}Cx_{16}C$ (catfish) or $CxCx_{28}Cx_{17}C$ (carp) or $CxCx_{28}Cx_{18}C$ (zebrafish)), but different from the LRRCT motifs of mouse Tlr11-13 ($CxCx_{24}Cx_{16\text{-}19}C$).

Table 3 Molecular characteristics of teleost Tlr20 and mouse Tlr11, Tlr12, and Tlr13

Name	aa lenght	Signal peptide	LRR	LRRNT	LRRCT
CcTlr20	946	22	26	$Cx_{14}Cx_8C$	$CxCx_{28}Cx_{17}C$
DrTlr20a	942	19	26	$Cx_{14}Cx_8C$	$CxCx_{28}Cx_{18}C$
DrTlr20b	943	19	26	$Cx_{23}C$	$CxCx_{28}Cx_{18}C$
DrTlr20c	951	25	26	$Cx_{23}C$	$CxCx_{28}Cx_{18}C$
DrTlr20d	949	24	26	$Cx_{14}Cx_8C$	$CxCx_{28}Cx_{18}C$
IpTlr20-1	933	18	26	$Cx_{14}Cx_8C$	$CxCx_{28}Cx_{16}C$
IpTlr20-2	351	NA	4	NA	$CxCx_{28}Cx_{16}C$
MmTlr11	931	35	25	$Cx_{17}Cx_{11}C$	$CxCx_{24}Cx_{19}C$
MmTlr12	906	19	24	$Cx_{17}Cx_{10}C$	$CxCx_{24}Cx_{19}C$
MmTlr13	991	NA	27	$Cx_{11}C$	$CxCx_{24}Cx_{16}C$

List of open reading frame (aa length), signal peptide, number of leucine rich repeats (LRR), and signature of leucine-rich N-terminal (LRRNT) and C-terminal (LRRCT) domains in common carp (*Cyprinus carpio*), zebrafish (*Danio rerio*), and channel catfish (*Ictalurus punctatus*) Tlr20 and mouse (*Mus musculus*) Tlr11, Tlr12, and Tlr13. Predicted Atlantic salmon (*Salmo salar*) Tlr20 was not include

Tlr, Toll-like receptor; *Cc*, *Cyprinus carpio*; *Dr*, *Danio rerio*, *Ip*, *Ictalurus punctatus*; *Mm*, *Mus musculus*; *NA*, not applicable

Conservation of synteny was investigated by comparing the genomic regions immediately up- and downstream of mouse *tlr11* on chromosome 14, mouse *tlr12* on chromosome 4 and mouse *tlr13* on the x chromosome with the genomic regions up- and downstream of the zebrafish *tlr20* genes on two regions of chromosome 9. For channel catfish, genome information on the immediate areas around *tlr20* is scarce (Quiniou and Waldbieser 2011) and could not be used to investigate synteny. For carp, although limited in length, genomic regions up- and downstream of *tlr20* (contig 28896; size, 20,020 bp) confirmed conservation of synteny with two genes (genes *slc10a2* and *gtpbp8*) in the region upstream of zebrafish *tlr20* (Fig. 4). Synteny analysis of the region flanking *tlr20* genes on zebrafish chromosome 9 did not reveal a conservation with genes directly flanking mouse *tlr11*, *tlr12*, or *tlr13*. However, we observed conservation of a block of six genes downstream of *tlr20a–d* on zebrafish chromosome 9 with a block of genes upstream of the *tlr11* gene on mouse chromosome 14 (Fig. 4). The conservation of this group of genes suggests that Tlr11 could be a possible ortholog of Tlr20.

Subcellular localization of Tlr20

To investigate the subcellular localization of Tlr20, we transfected human HEK 293 and fish EPC and CLC cell lines with HA-tagged carp Tlr20-GFP (HA-Tlr20-GFP; Fig. 5). Only in permeabilized cells, the presence of the HA-Tlr20 could be visualized (Fig. 5b), suggesting a preferential expression of Tlr20 in intracellular compartments in all three cell lines studied. To further investigate the subcellular localization of Tlr20, we cotransfected HA-Tlr20-GFP-transfected

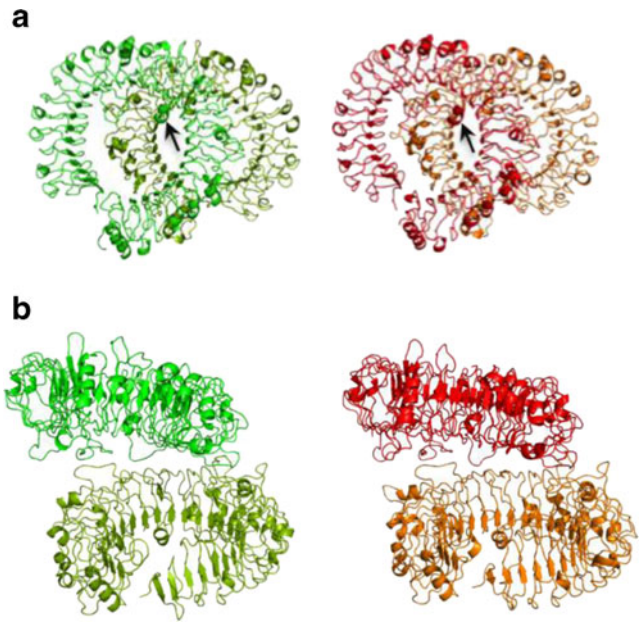

Fig. 2 Three-dimensional structure of Tlr20 shows a best fit to human TLR8. **a** Frontal view and **b** top view of carp Tlr20 (*green*) and human TLR8 (*red*). Three-dimensional model for carp Tlr20 based on the crystal structure of human TLR8 (PDB-id: 3w3g). Carp Tlr20 is shown as a homodimer on the left panels (*bright* and *dark green* for each monomer); human TLR8 as a homodimer on the *right panels* (*bright* and *dark red* for each monomer). The loop between LRR15 and LRR16 is indicated with a *black arrow*

ZF4 cells with a plasmid encoding for KDEL-RFP protein for specific localization to the ER (Fig. 5c). Colocalization of KDEL-RFP with Tlr20-GFP confirmed a preferential expression of Tlr20 in intracellular compartments and suggested subcellular localization to the ER.

In vitro ligand binding of Tlr20

To investigate the putative ligands of Tlr20, we developed a reporter assay based on a human (HEK 293) cell line stably transfected with a NF-κB luciferase reporter construct (HEK-pNiFty-Luc) and transiently transfected with carp Tlr20. We used transient transfection with human TLR2 as positive control. Successful transfection was confirmed by microscopy, evaluating the percentage of fluorescent cells (40–50 % approximately) by visualizing GFP for carp Tlr20 or YFP for human TLR2. Responses to ligands were measured as luminescence and expressed as relative light units. Stimulation with human tumor necrosis factor alpha (TNF-α) induced a very high response in HEK-NFκB-Luc cells transiently transfected with empty plasmid, human TLR2 or carp Tlr20. Overexpression of human TLR2 and stimulation with a prototypical TLR2 ligand, Pam_2CSK_4, also induced a very high and specific luminescence response. However, stimulation of cells overexpressing carp Tlr20 with profillin (*T. gondii*-derived ligand of murine Tlr11 and Tlr12) did not lead to activation of the NF-κB promotor (Fig. 6). Stimulation of these cells with other prototypical TLR ligands (LPS-PG, LPS-EB, and LTA), *E. coli* single-strand DNA, CpG, and Poly (I:C), flagellin, and 23S rRNA (ORN Sa19) also did not lead to activation of the NF-κB promotor (data not shown).

In vivo modulation of *tlr20* gene expression after parasitic infection

In vitro studies could not clearly identify a ligand for carp Tlr20, for which reason we examined biological sample collections from both zebrafish and carp for *tlr20* gene expression during infection with bacterum, virus, or parasite. Using existing material (Hegedűs et al. 2009; Veneman et al. 2013), we mapped the reads of RNAseq experiments on the zebrafish *tlr20* transcripts. Zebrafish *tlr20a–d* are transcribed during both larval and adult stages but at very low levels, close to the detection limit. Based on reads linked to the polymorphic regions, we can conclude that all full length copies have a detectable, although low transcription level. Since the *tlr20* copies are extremely similar to each other, a majority of the mapped reads could not be assigned to a particular *tlr20* transcript, and thus, a specific induction of one of the copies of *tlr20* could not be discerned and is technically not possible with the current standards of sequencing depth. We could not obtain evidence for an induction of any of the *tlr20* copies by infection with *Mycobacterium marinum* or *Staphylococcus epidermis* bacteria (data not shown). *Tlr20* was also not significantly modulated in biological sample collections taken after viral infection of carp with spring viraemia of carp virus (SVCV) (Forlenza et al. 2008a). In contrast, infection of carp with the blood parasite *T. borreli* (Forlenza et al. 2008b), induced a clear two- to sixfold upregulation of *tlr20* gene expression 6 weeks after infection (late stage of infection), at least in head kidney, spleen, and in PBLs (Fig. 7). Similarly, infection with *T. carassii* (Joerink et al. 2006), a related blood parasite of carp, induced a clear two- to fourfold upregulation of *tlr20* gene expression at 6–8 weeks after infection (data not shown). These data seem to support a role for *tlr20* in the immune response to parasitic rather than bacterial or viral infections.

Modulation of *tlr20* gene expression by parasite lysate

Parasite-induced gene expression of *tlr20* was high in head kidney, spleen, and PBL. Constitutive gene expression of *tlr20* was examined in a tissue and leukocyte cDNA library of naive carp. A relatively high constitutive gene expression level of carp *tlr20* was observed in several organs, especially in gut and PBL (Fig. 8a). Furthermore, constitutive gene expression of carp *tlr20* was particularly high in B lymphocytes sorted from PBL (Fig. 8b). Although in vitro stimulation with parasite (*T. borreli*) lysate of HEK-pNiFty-Luc cells transiently transfected with carp Tlr20 did not lead to cell

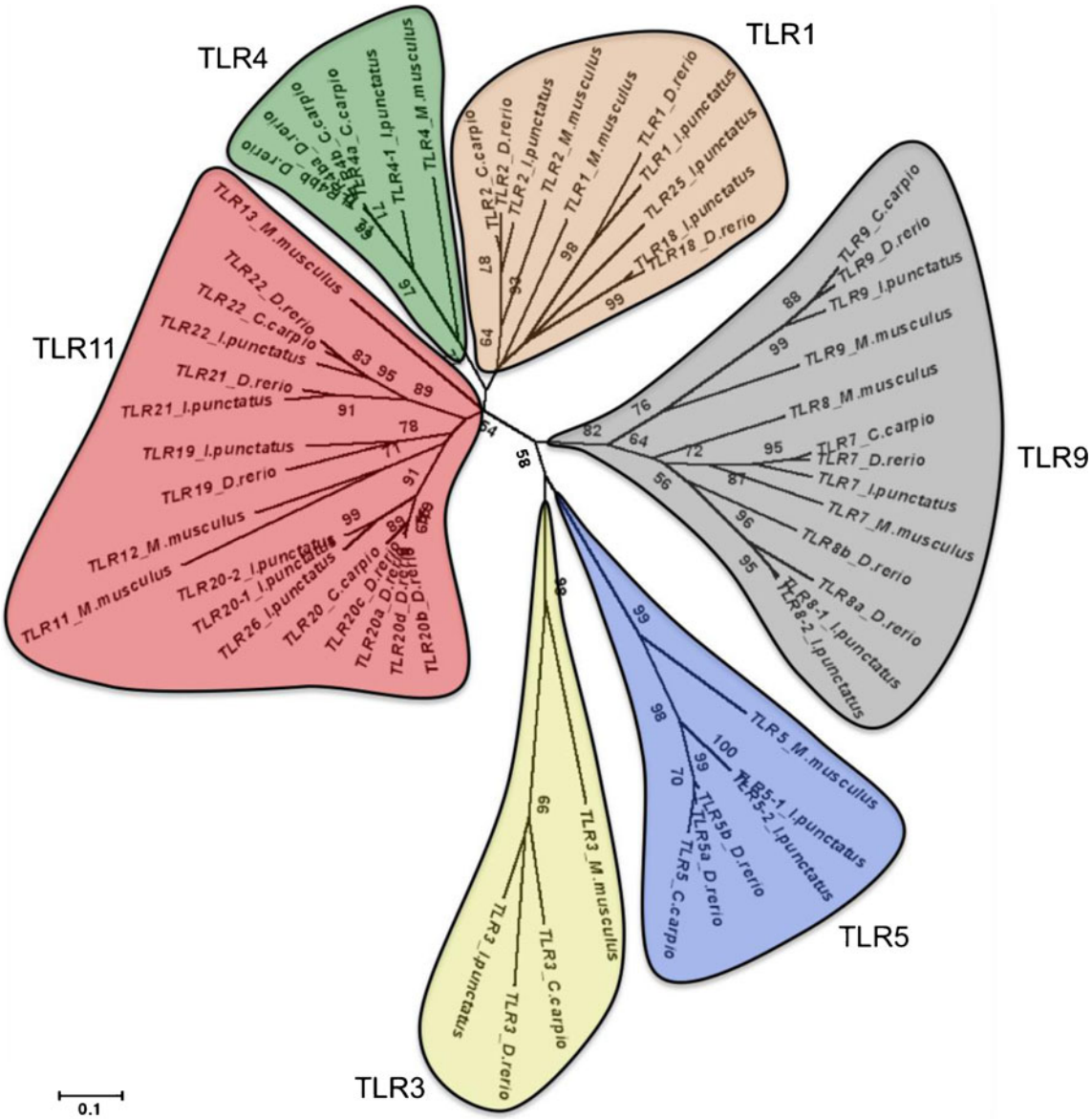

Fig. 3 Phylogenetic analysis of Tlr20 shows clustering with Tlr11 family members Tlr11 and Tlr12. Neighbor-joining tree based on amino acid identities in the TIR domains of Tlrs from carp, zebrafish, channel catfish, and mouse. Phylogenetic analysis was conducted with 10,000 bootstrap replicates; bootstrap values at major branching points are shown as percentages. The sequences were derived from *Cyprinus carpio* (Tlr2, ACP20793; Tlr3, ABL11473; Tlr4a, ADC45015; Tlr4b, ADY76945; Tlr5, AGH15501; Tlr7, BAJ19518; Tlr9, ADC45018; Tlr20, KF482527; Tlr22, ADR66025); *Danio rerio* (Tlr1, AAI63271; Tlr2, AAQ90474; Tlr3, NP_001013287; Tlr4ba, ACE74929; Tlr4bb, NP_997978; Tlr5a, XP_001919052; Tlr5b, NP_001124067; Tlr7, XP_003199309; Tlr8a, XP_001920594; Tlr8b, XP_001340186; Tlr9, NP_001124066; Tlr18, AAI63840; Tlr19, XP_002664892; Tlr20a, ENSDARG00000094411; Tlr20b, ENSDARG00000092668; Tlr20c, ENSDARG00000041164; Tlr20d, ENSDARG00000088701; Tlr21, NP_001186264; TLR22, AAI63527); *Ictalurus punctatus* (Tlr1, AEI59662; Tlr2, AEI59663; Tlr3, AEI59664; Tlr4-1, AEI59665; TLR5S, AEI59667; Tlr5-1, AEI59668; Tlr5-2, AEI59669; Tlr7, AEI59670; Tlr8-1, AEI59671; Tlr8-2, AEI59672; Tlr9, AEI59673; Tlr18, AEI59674; Tlr19, AEI59675; Tlr20-1, AEI59676; Tlr20-2, AEI59677; Tlr21, AEI59678; Tlr22, AEI59679; Tlr25, AEI59680; Tlr26, AEI59681); *Mus musculus* (Tlr1, NP_001263374; Tlr2, AAD46481; Tlr3, NP_569054; Tlr4, AAD29272; Tlr5, NP_058624; Tlr7, AAL73191; Tlr8, AAK62677; Tlr9, AAK28488; Tlr11, AAS37672; Tlr12, AAS37673; Tlr13, AAS37674)

activation (data not shown), in vitro stimulation of PBL from naive fish with *T. borreli* lysate induced a clear (threefold) upregulation of *tlr20* (Fig. 8c). In addition, in vitro restimulation of PBL from carp that survived a *T. borreli* infection with *T. borreli* lysate also induced a clear (threefold) upregulation of *tlr20* (data not shown).

Discussion

The complexity of the Toll-like receptor family still is increasing, owing to the continuous discovery of additional members that do not seem to have clear homologues to mammalian TLRs. Apparently, there are several Tlrs that have been lost

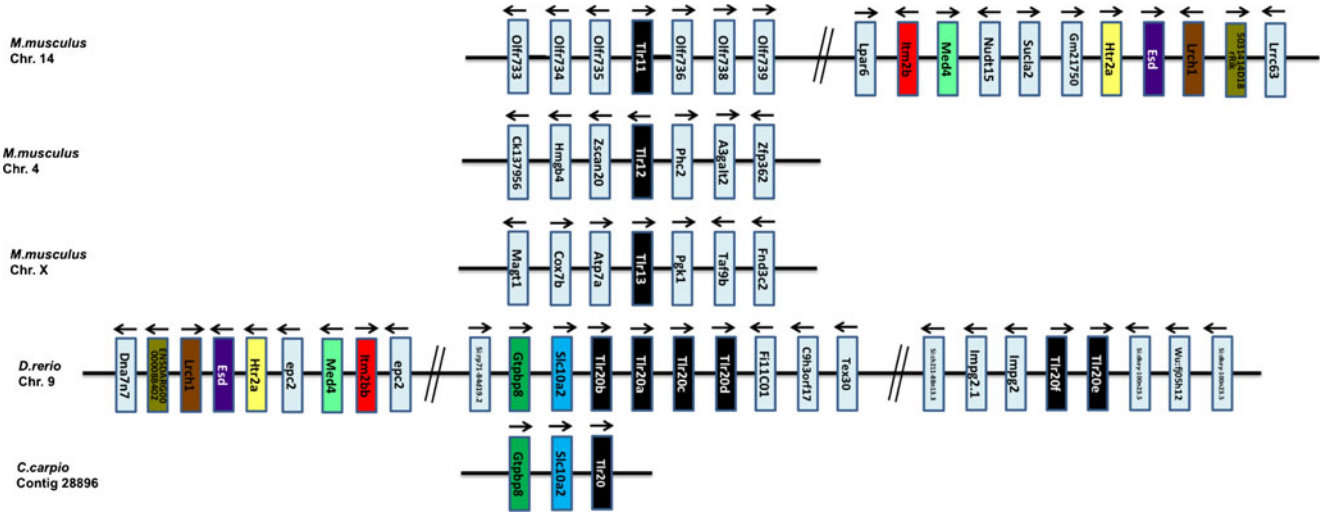

Fig. 4 Comparison of genomic regions carrying mouse Tlr11 family members Tlr11, Tlr12, and Tlr13 and teleost Tlr20. Comparative maps of genomic regions linked to *tlr11* (mouse chromosome 14, regions 50139702–50643369 and 73237891–75130881 bp), *tlr12* (chromosome 4, region 127243784–129122036 bp), *tlr13* (chromosome X, region 105079756–107104974 bp), zebrafish *tlr20* (chromosome 9, regions 26476439–25984474 and 27137159–31418367 bp) and carp *tlr20* (contig 28896). For the mouse, genome assembly PRJNA73579 was used. For zebrafish, genome assembly GCA_000002035 was used. Similar colors indicate the possibility of orthology

during evolution and are not present in mammals but are present in reptiles, amphibians, and/or fish (Boyd et al. 2012; Ishii et al. 2007; Palti 2011; Quiniou et al. 2013). Tlr20 is a nonmammalian Tlr the function of which is unknown. Conservation of genes on zebrafish chromosome 9, which carries *tlr20*, with genes on mouse chromosome 14, which carries *tlr11*, indicates Tlr11 could be a possible ortholog of Tlr20.

We identified full-length cDNA sequences for *tlr20* of both zebrafish and common carp, two closely related cyprinid fish species. Previously, full-length cDNA sequences for *tlr20* had only been described for channel catfish (Quiniou et al. 2013), a fish species that is among the closest living relatives to the cyprinids. Catfish Tlr20 is found in two copies as a close proximity tandem duplication in the catfish genome. At present, it is not clear if the second, shorter gene (*tlr20*-2) encodes a functional protein (Quiniou et al. 2013). Although salmonid fish also appear to express Tlr20; at least in rainbow trout, a partial *tlr20* EST has been identified (Palti et al. 2006) and a *tlr20* sequence has been retrieved from a whole genome shotgun sequencing of Atlantic salmon (Quiniou et al. 2013), attempts to retrieve *tlr20* from other teleost groups have failed so far.

In silico analysis of a previous version of the zebrafish genome (ZV2) predicted six *tlr20* sequences with some found as close proximity tandem duplications on chromosome 9 (Meijer et al. 2004). The first gene expression studies with reverse transcriptase PCR suggested that at least two *tlr20* genes in zebrafish were expressed and modulated by mycobacterium infection (Meijer et al. 2004). We confirmed the presence of six zebrafish *tlr20* genes in the latest assembly of the zebrafish genome (ZV9), but found that two copies (*tlr20e* and *tlr20f*) in the genome contain mutations in the reading frame that are not leading to the expected products, in one case leading to a premature stop codon. The four full-length zebrafish *tlr20* all have a signal peptide. Zebrafish *tlr20* displayed a low constitutive gene expression level, which was not significantly modulated upon infection with *M. marinum* or *S. epidermis*, at least not to an extent detectable by RNAseq.

Surprisingly, in common carp, which is a very close relative of zebrafish, we could detect only a single *tlr20* sequence in the genome. This is surprising because, usually in the tetraploid carp, genes are found as duplicated copies of those found in diploid zebrafish (Henkel et al. 2012). Although it cannot be excluded that some mistakes are present in the current assembly of the carp genome, it is highly unlikely that up to a number of 11 possible copies of the carp *tlr20* genes would have been missed during the assembly.

Sequence analyses place teleost Tlr20 in the TLR11 family, which also comprises three Tlrs unique to mouse: Tlr11, Tlr12, and Tlr13, characterized by 25, 26, or 27 LRRs, respectively (Matsushima et al. 2007). Assumed important for the recognition of PAMPs, the extracellular domain of Tlr20 molecules from carp, zebrafish, and catfish (Tlr20-1) all have an identical number of 26 LRRs. Assumed important for protection of the hydrophobic core of the first LRR (Park et al. 2008), the $Cx_{14}Cx_8C$ LRRNT motif is the same among all teleost Tlr20 molecules, but different from the LRRNT motifs found in mouse Tlr11-13. Assumed important for protection of the hydrophobic core of the last LRR, the $CxCx_{28}Cx_{16-18}C$ LRRCT motif is similar, although not exactly the same, in the teleost Tlr20 molecules and comparable to the LRRCT motifs found in mouse Tlr11–13 ($CxCx_{24}Cx_{16-19}C$). These molecular

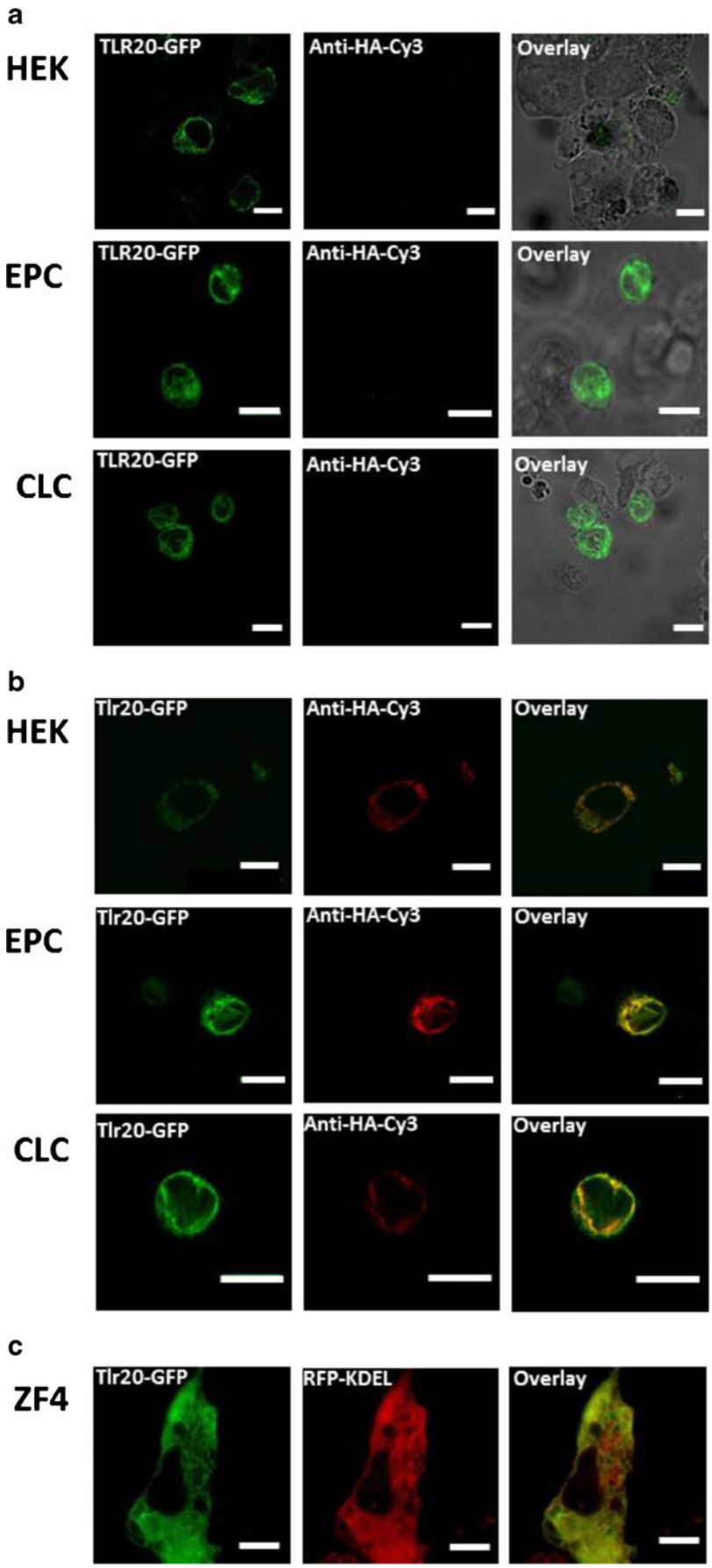

Fig. 5 Tlr20 preferentially locates intracellularly at the endoplasmatic reticulum (ER). **a** Nonpermeabilized cells. **b** Permeabilized cells. **c** Cell cotransfected with KDEL-RFP for localization to the ER. **a**, **b** Confocal microscopy of HEK 293, EPC, and CLC cells overexpressing carp Tlr20. Cells were seeded 24 h prior to transfection with HA-Tlr20-GFP. Three days later, cells were either permeabilized or left untreated and stained for microscopy using mouse anti-HA and donkey antimouse Cy3 antibodies. *Left panels* Tlr20-GFP (*green*); *middle panels* recognition of HA-tagged proteins (*red*); *right panels* overlay (*yellow-orange*). **c** Confocal microscopy of ZF4 cells overexpressing carp Tlr20. Subcellular localization to the ER was examined in live cells 2 days after transfection with KDEL-RFP. *Left* Tlr20-GFP (*green*); *middle* KDEL-RFP (*red*); *right* overlay (*yellow-orange*). Bar=10 μm

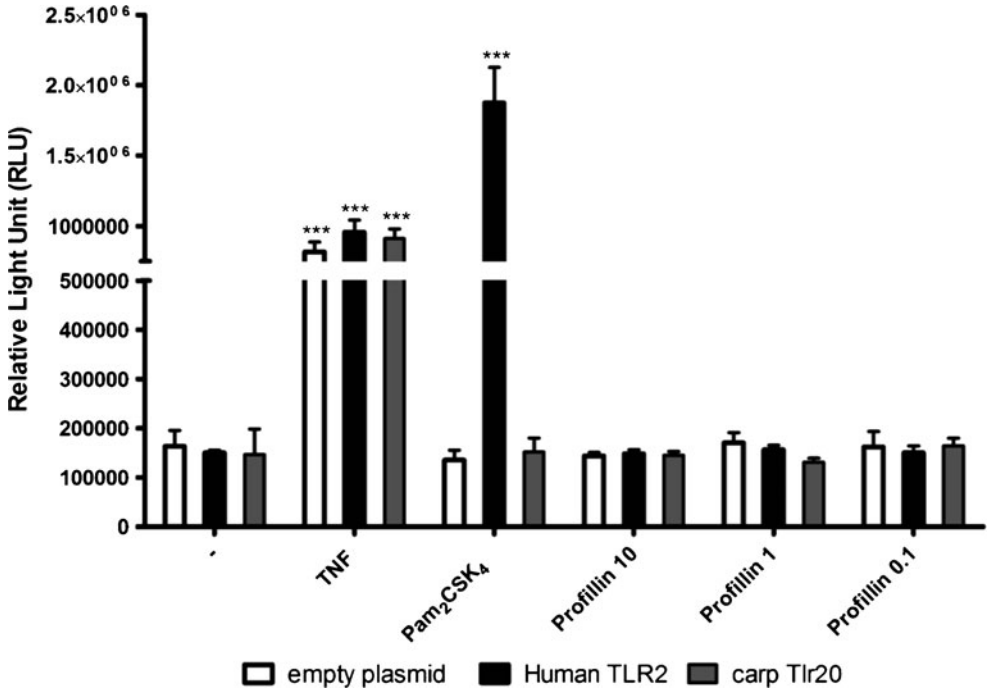

Fig. 6 In vitro ligand-binding studies do not clearly identify a ligand for Tlr20. Reporter HEK-NFκB-Luc cells were transiently transfected with empty plasmid (pcDNA3-GFP) or with plasmid coding for human TLR2-YFP or carp HA-Tlr20-GFP. After 72 h, transiently transfected cells were stimulated with PBS, human TNF (200 ng/ml), Pam_2CSK_4 (20 μg/ml), or profillin (10, 1, 0.1 μg/ml) from *Toxoplasma gondii* for 5 h. After stimulation, luminescence was measured in cell lysates and expressed as relative light units. Values represent mean±SD of triplicate wells of one representative experiment out of three independent experiments. Significant differences with respect to the control (empty plasmid) are indicated with an *asterisk* (***$P<0.001$)

characteristics not only suggest that Tlr20 fits well the TLR11 family but also point at differences between teleost Tlr20 and Tlr11 family members found in the mouse.

Conservation of synteny was observed between a region downstream of the *tlr20a–d* genes on zebrafish chromosome 9 with a region upstream of *tlr11* on mouse chromosome 14 (and with a region upstream of *tlr11* on rat chromosome 15; unpublished data). The conservation of this group of genes suggests that Tlr11 could be a possible ortholog of Tlr20. Also of interest, *tlr19* is close to two genes: *s100a10b* (ENSDARG00000025254) and *slc50a1* (ENSDARG00000015158) on zebrafish chromosome 16, for which possible orthologs can be found on chromosome 15 of the rat (*Rattus norvegicus*) (ENSRNOG00000010144; 107,614,426-107,614,863, ortholog of *s100a10b*) that also carries *tlr11*, and on rat chromosome 5 (ENSRNOG00000015706; 169,975,662-169,977,253, ortholog of *slc50a1*) that also carries *tlr12*. This is interesting because of the close phylogenetic relationship between Tlr20 and Tlr19 (see Fig. 3). Overall, synteny analysis of the zebrafish genome suggests that Tlr11 could be a possible ortholog of Tlr20. Three-dimensional modeling based on the crystal structure of human TLR8, an intracellular TLR that senses RNA, showed a similar structure for all teleost Tlr20 molecules characterized by a slight distortion of the horseshoe shape the effect of which, if any, is unknown. TLRs can be expressed in different compartments of the cell: on the cell surface, in intracellular vesicles such as endosomes, or as part of the ER. TLRs can also translocate from one compartment to another. Our confocal microscopic analysis of Tlr20 suggested a possible subcellular localization of Tlr20 in the ER.

In vitro reporter assays based on NF-κB activation following overexpression of carp Tlr20 in human cell lines, or fish cell lines (EPC and CLC, data not shown), could not identify a ligand unique to Tlr20. It could be that the cell lines used represent cell types that could not fully support natural subcellular localization, ligand binding, and/or Tlr20 signaling. Such an observation has been made for salmon Tlr9, which, when overexpressed in salmonid cell lines, failed to translocate to CpG-containing endosomes. Apparently, only specific immune cell types in salmon have the ability to relocate the Tlr9 receptor to the appropriate cellular compartments where it may become activated by its ligand (Iliev et al. 2013). UNC93B1 is a transmembrane protein required for TLR3, TLR7, TLR9, TLR11, TLR12, and TLR13 function, which controls trafficking from the ER to endolysosomes. UNC93B1 remains associated with TLRs through post-Golgi sorting steps, but these steps are different among endosomal TLRs. For example, TLR9 requires UNC93B1-mediated recruitment of adaptor protein complex 2 for delivery to endolysosomes, whereas TLR7, TLR11, TLR12, and TLR13 use alternative trafficking pathways. Thus, endosomal TLRs are differentially sorted by UNC93B1 (Lee et al. 2013). Despite the identification of a sequence encoding for a *unc93b1* homologue in teleosts (Pietretti et al. 2013), it cannot be excluded that this molecule, or other accessory molecules (Lee et al. 2012), crucial to the natural function of Tlr20 could be too different, or absent, in the (human or fish) cell lines used. Indeed, a preliminary investigation of the transcriptome of the EPC fish cell line suggests these cells do not express *unc93b1* (Pietretti, unpublished data). The apparent absence of *unc93b1* from the EPC transcriptome could maybe have

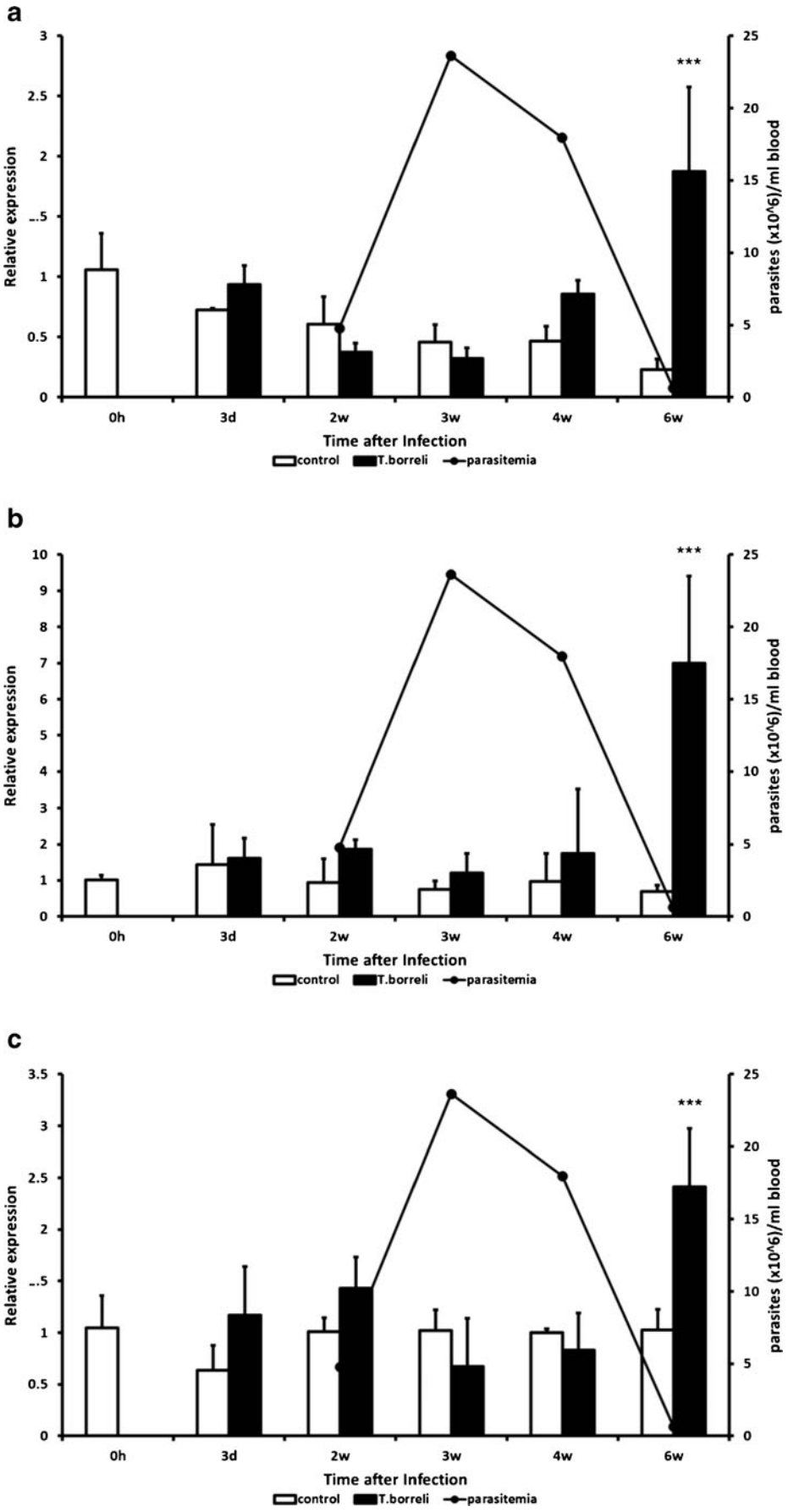

Fig. 7 In vivo infection with parasites induces upregulation of *tlr20* gene expression in carp. Gene expression profiles after infection with *T. borreli* in **a** head kidney, **b** spleen, and **c** peripheral blood leukocytes (*PBL*). Carp were injected with 1×10^4 *Trypanoplasma borreli* parasites per fish, or with PBS (negative control). Organs were collected from $n=5$ infected and $n=3$ noninfected fish at each time point, over a period of 6 weeks. Parasitemia (*T. borreli*/ml blood) is shown as a *line graph*. Relative gene expression was normalized to the reference gene and expressed relative to the controls at time point zero and is shown as *bar graphs*. *White* bars represent noninfected control, and *black bars* represent *T. borreli*-infected carp. Values are mean±SD of $n=3$–5 fish. Significant differences to the time point control are indicated with an *asterisk* (***$P<0.001$)

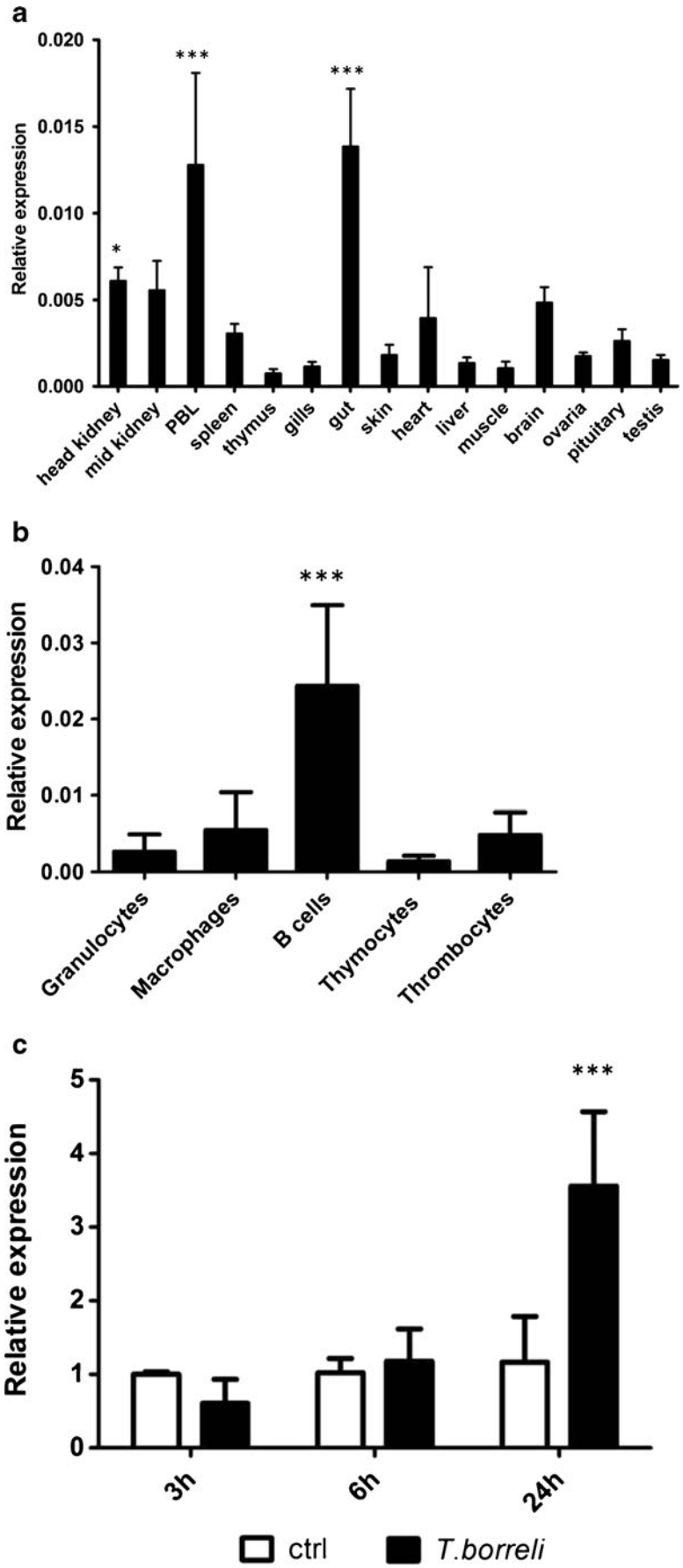

Fig. 8 Peripheral blood leukocytes (*PBL*) of carp express relatively high basal *tlr20* gene expression levels that can be upregulated by parasites. Gene expression profiles in **a** organs from naive fish, **b** leukocyte cell populations from naïve fish and **c** PBL stimulated in vitro with parasite lysate. **a**, **b** Constitutive mRNA levels of *tlr20* in different organs and different leukocyte cell populations of carp. **c** Induced mRNA levels of *tlr20* in PBL of naive fish stimulated in vitro with *T. borreli* parasite lysate (equivalent of 1:2 parasites/cells). Relative gene expression was normalized to the reference gene and is shown as *bar graphs*. Significant differences were calculated in comparison with the lowest expressed values in thymus (**a**) or thymocytes (**b**). *Bars* represent mean±SD of $n=3$–5 healthy carp (**a**, **b**) or triplicate wells of one representative experiment out of three independent experiments. Significant differences were calculated using one-way ANOVA and are indicated by *asterisks* (*$P<0.01$) and ***$P<0.001$)

affected the functional characterization of Tlr20 overexpressed in this particular cell line.

Phylogenetic analyses place Tlr20 closest to Tlr11 and Tlr12 of the TLR11 family, two TLRs that sense ligands from protozoan parasites (*T. gondii*) in the mouse. Only few studies have looked at the expression of Tlr20 in vivo. Initial studies in whole zebrafish embryos infected with *M. marinum* (Meijer et al. 2004) suggested increased expression of *tlr20a* 8 weeks after intraperitoneal injection of bacteria. In adult channel catfish, infection with *E. ictaluri* led to increased expression of *tlr20* 6 h after injection (Pridgeon et al. 2010). We reexamined biological sample collections from both zebrafish and carp for *tlr20* gene expression. Infection of zebrafish with *S. epidermis* (Veneman et al. 2013) and with *M. marinum* (Hegedűs et al. 2009) did not clearly modulate *tlr20* gene expression. Infection of carp with SVCV (Forlenza et al. 2008a) did not significantly modulate *tlr20* gene expression after bath challenge with this virus. In contrast, infection of carp with the blood parasite *T. borreli* (Forlenza et al. 2008b), induced a clear upregulation of *tlr20* gene expression after the peak of parasitemia, at 6 weeks after infection. Moreover, we observed a similar upregulation of *tlr20* at 6–8 weeks postinfection with a related blood parasite of carp, *T. carassii* (data not shown). Subsequent analysis of constitutive gene expression in different organs and leukocyte cell types confirmed a high constitutive expression of *tlr20* in PBL and in B lymphocytes sorted from PBL. We looked in more detail at *tlr20* gene expression induced by *T. borreli*. Stimulation of PBL from naive fish with *T. borreli* lysate induced a clear upregulation of *tlr20*. Restimulation of PBL from fish that had survived a *T. borreli* infection also induced a clear upregulation of *tlr20*. In humans, immature transitional B cells and naive B cells exhibit some responses to Tlr ligands, in particular CpG-containing oligodinucleotides, but exhibit strong responses when simultaneously stimulated *via* the B cell receptor and CD40. IgM-positive memory B cells also exhibit strong responses to Tlr ligands (DeFranco et al. 2012). In future experiments, it would be of interest to study the role of Tlr20 in fish B lymphocytes and study a putative effect of B cell receptor co-stimulation on *tlr20* gene expression.

Although our data suggest that Tlr20 may play a role in the immune response to trypanosomes, it is difficult to define a clear ligand for Tlr20 based on our in vivo studies. In general, the subcellular localization of TLRs often corresponds to the place at which recognition of particular PAMPs occurs; TLRs expressed at the cell surface generally recognize outer membrane components of microbes such as lipids and (lipo)proteins, whereas TLRs expressed intracellularly recognize microbial nucleic acids (Kawai and Akira 2010). The intracellular localization of Tlr20 could point at a nucleic acid type of ligand or pathogen-derived protein produced in the host. Our in vitro reporter assays could not clearly identify a ligand for Tlr20. Future studies could take into account accessory proteins present or absent in cell lines used for in vitro studies. Such accessory molecules can be divided based on their functions as mediators of ligands delivery and/or recognition, chaperones, trafficking, or TLR processing factors (Lee et al. 2012). The identification of several, although not all, accessory molecules in fish (Pietretti et al. 2013) may allow for combined studies on Tlr molecules and accessory molecules and may shed further light on the function of fish-specific TLRs such as Tlr20.

Acknowledgments Carla Maria Piazzon, Alberto Falco and Anders Østergaard are gratefully acknowledged for their technical support and their fruitful discussions. Adrie Westphal from the laboratory of Biochemestry, Department of Agrotechnology and Food Sciences at Wageningen University, The Netherlands, is gratefully acknowledged for the three-dimensional modeling of carp Tlr20. The authors would like to thank the unknown reviewer for useful information on conservation of synteny. The research leading to these results has received funding from the European Commission under the 7th Framework Programme for Research and Technological Development (FP7) of the European Union (grant agreements NEMO PITN-GA-2008-214505, FishForPharma PITN-GA-2011-289209, and TARGETFISH 311993).

References

Akira S, Uematsu S, Takeuchi O (2006) Pathogen recognition and innate immunity. Cell 124:783–802

Altschul SF, Gish W, Miller W, Myers EW, Lipman DJ (1990) Basic local alignment search tool. J Mol Biol 215:403–410

Ariffin JK, Sweet MJ (2013) Differences in the repertoire, regulation and function of Toll-like receptors and inflammasome-forming Nod-like receptors between human and mouse. Curr Opin Microbiol 16:303–310

Baoprasertkul P, Xu P, Peatman E, Kucuktas H, Liu Z (2007) Divergent Toll-like receptors in catfish (*Ictalurus punctatus*): TLR5S, TLR20, TLR21. Fish Shellfish Immunol 23:1218–1230

Bell JK, Mullen GE, Leifer CA, Mazzoni A, Davies DR, Segal DM (2003) Leucine-rich repeats and pathogen recognition in Toll-like receptors. Trends Immunol 24:528–533

Benson DA, Boguski MS, Lipman DJ, Ostell J, Ouellette B, Rapp BA, Wheeler DL (1999) GenBank. Nucleic Acids Res 27:12

Boyd AC, Peroval MY, Hammond JA, Prickett MD, Young JR, Smith AL (2012) TLR15 is unique to avian and reptilian lineages and recognizes a yeast-derived agonist. J Immunol 189:4930–4938

Brownlie R, Allan B (2011) Avian toll-like receptors. Cell Tissue Res 343:121–130

Brownlie R, Zhu J, Allan B, Mutwiri GK, Babiuk LA, Potter A, Griebel P (2009) Chicken TLR21 acts as a functional homologue to mammalian TLR9 in the recognition of CpG oligodeoxynucleotides. Mol Immunol 46:3163–3170

DeFranco AL, Rookhuizen DC, Hou B (2012) Contribution of Toll-like receptor signaling to germinal center antibody responses. Immunol Rev 247:64–72

Driever W, Rangini Z (1993) Characterization of a cell line derived from zebrafish (*Brachydanio rerio*) embryos. In Vitro Cell Dev Biol Anim 29:749–754

Eswar N, Webb B, Marti-Renom MA, Madhusudhan M, Eramian D, Shen M-y, Pieper U, Sali A (2006) Comparative protein structure modeling using Modeller. Curr Protoc Bioinforma 5.6.1–5.6.30

Faisal M, Ahne W (1990) A cell line (CLC) of adherent peripheral blood mononuclear leucocytes of normal common carp *Cyprinus carpio*. Dev Comp Immunol 14:255–260

Fijan N, Sulimanović D, Bearzotti M, Muzinić D, Zwillenberg L, Chilmonczyk S, Vautherot J, De Kinkelin P (1983) Some properties of the Epithelioma papulosum cyprini (EPC) cell line from carp *Cyprinus carpio*. Elsevier/Annales de l'Institut Pasteur/Virologie, Amsterdam

Flicek P, Amode MR, Barrell D, Beal K, Brent S, Carvalho-Silva D, Clapham P, Coates G, Fairley S, Fitzgerald S (2012) Ensembl 2012. Nucleic acids Res 40:D84–D90

Forlenza M, Dias JD, Veselý T, Pokorová D, Savelkoul HF, Wiegertjes GF (2008a) Transcription of signal-3 cytokines, IL-12 and IFNαβ, coincides with the timing of CD8αβ up-regulation during viral infection of common carp (*Cyprinus carpio* L.). Mol Immunol 45: 1531–1547

Forlenza M, Scharsack JP, Kachamakova NM, Taverne-Thiele AJ, Rombout JH, Wiegertjes GF (2008b) Differential contribution of neutrophilic granulocytes and macrophages to nitrosative stress in a host–parasite animal model. Mol Immunol 45:3178–3189

Forlenza M, Kaiser T, Savelkoul H, Wiegertjes GF (2012) The use of real-time quantitative PCR for the analysis of cytokine mRNA levels. Methods Mol Biol 820:7 (Clifton, NJ)

Gasteiger E, Gattiker A, Hoogland C, Ivanyi I, Appel RD, Bairoch A (2003) ExPASy: the proteomics server for in-depth protein knowledge and analysis. Nucleic acids Res 31:3784–3788

Hegedűs Z, Zakrzewska A, Ágoston VC, Ordas A, Rácz P, Mink M, Spaink HP, Meijer AH (2009) Deep sequencing of the zebrafish transcriptome response to mycobacterium infection. Mol Immunol 46:2918–2930

Henkel CV, Dirks RP, Jansen HJ, Forlenza M, Wiegertjes GF, Howe K, van den Thillart GE, Spaink HP (2012) Comparison of the Exomes of Common Carp (*Cyprinus carpio*) and Zebrafish (*Danio rerio*). Zebrafish 9:59–67

Iliev DB, Skjæveland I, Jørgensen JB (2013) CpG oligonucleotides bind TLR9 and RRM-containing proteins in Atlantic salmon (*Salmo salar*). BMC Immunol 14:1–12

Irnazarow I (1995) Genetic variability of Polish and Hungarian carp lines. Aquaculture 129:215–219

Ishii A, Kawasaki M, Matsumoto M, Tochinai S, Seya T (2007) Phylogenetic and expression analysis of amphibian *Xenopus* Toll-like receptors. Immunogenetics 59:281–293

Joerink M, Forlenza M, Ribeiro C, de Vries BJ, Savelkoul HF, Wiegertjes GF (2006) Differential macrophage polarisation during parasitic infections in common carp (*Cyprinus carpio* L.). Fish Shellfish Immunol 21:561–571

Kawai T, Akira S (2010) The role of pattern-recognition receptors in innate immunity: update on Toll-like receptors. Nat Immunol 11: 373–384

Keestra AM, de Zoete MR, van Aubel RA, van Putten JP (2007) The central leucine-rich repeat region of chicken TLR16 dictates unique ligand specificity and species-specific interaction with TLR2. J Immunol 178:7110–7119

Koblansky AA, Jankovic D, Oh H, Hieny S, Sungnak W, Mathur R, Hayden Matthew S, Akira S, Sher A, Ghosh S (2013) Recognition of profilin by Toll-like receptor 12 is critical for host resistance to *Toxoplasma gondii*. Immunity 38:119–130

Koumans-van Diepen JE, Egberts E, Peixoto BR, Taverne N, Rombout JH (1995) B cell and immunoglobulin heterogeneity in carp (Cyprinus carpio L); An immuno (cyto) chemical study. Dev Comp Immunol 19:97–108

Lee CC, Avalos AM, Ploegh HL (2012) Accessory molecules for Toll-like receptors and their function. Nat Rev Immunol 12:168–179

Lee BL, Moon JE, Shu JH, Yuan L, Newman ZR, Schekman R, Barton GM (2013) UNC93B1 mediates differential trafficking of endosomal TLRs. eLife 2

Letunic I, Doerks T, Bork P (2012) SMART 7: recent updates to the protein domain annotation resource. Nucleic Acids Res 40:D302–D305

Matsuo A, Oshiumi H, Tsujita T, Mitani H, Kasai H, Yoshimizu M, Matsumoto M, Seya T (2008) Teleost TLR22 recognizes RNA duplex to induce IFN and protect cells from birnaviruses. J Immunol 181:3474–3485

Matsushima N, Tanaka T, Enkhbayar P, Mikami T, Taga M, Yamada K, Kuroki Y (2007) Comparative sequence analysis of leucine-rich repeats (LRRs) within vertebrate toll-like receptors. BMC Genomics 8:124

Medzhitov R, Preston-Hurlburt P, Janeway CA (1997) A human homologue of the *Drosophila* Toll protein signals activation of adaptive immunity. Nature 388:394–397

Meijer AH, Gabby KS, Medina RI, He S, Bitter W, Ewa S-JB, Spaink HP (2004) Expression analysis of the Toll-like receptor and TIR domain adaptor families of zebrafish. Mol Immunol 40:773

Nielsen H, Engelbrecht J, Brunak S, Von Heijne G (1997) Identification of prokaryotic and eukaryotic signal peptides and prediction of their cleavage sites. Protein Eng 10:1–6

Oldenburg M, Kruger A, Ferstl R, Kaufmann A, Nees G, Sigmund A, Bathke B, Lauterbach H, Suter M, Dreher S (2012) TLR13 recognizes bacterial 23S rRNA devoid of erythromycin resistance-forming modification. Sci Signal 337:1111

Oshiumi H, Tsujita T, Shida K, Matsumoto M, Ikeo K, Seya T (2003) Prediction of the prototype of the human Toll-like receptor gene family from the pufferfish, *Fugu rubripes*, genome. Immunogenetics 54:791–800

Palti Y (2011) Toll-like receptors in bony fish: from genomics to function. Dev Comp Immunol 35:1263–1272

Palti Y, Rodriguez M, Vallejo R, Rexroad C (2006) Mapping of Toll-like receptor genes in rainbow trout. Anim Genet 37:597–598

Park H, Huxley-Jones J, Boot-Handford R, Bishop P, Attwood T, Bella J (2008) LRRCE: a leucine-rich repeat cysteine capping motif unique to the chordate lineage. BMC Genomics 9:599

Pearson WR, Lipman DJ (1988) Improved tools for biological sequence comparison. Proc Natl Acad Sci 85:2444–2448

Pfaffl MW (2001) A new mathematical model for relative quantification in real-time RT-PCR. Nucleic Acids Res 29:e45

Pfaffl MW, Tichopad A, Prgomet C, Neuvians TP (2004) Determination of stable housekeeping genes, differentially regulated target genes and sample integrity: BestKeeper–Excel-based tool using pair-wise correlations. Biotechnol lett 26:509–515

Pietretti D, Spaink HP, Falco A, Forlenza M, Wiegertjes GF (2013) Accessory molecules for Toll-like receptors in teleost fish. Identification of TLR4 interactor with leucine-rich repeats (TRIL). Mol Immunol 56:745–756

Pridgeon J, Russo R, Shoemaker C, Klesius P (2010) Expression profiles of toll-like receptors in anterior kidney of channel catfish, *Ictalurus punctatus* (Rafinesque), acutely infected by *Edwardsiella ictaluri*. J Fish Dis 33:497–505

Quiniou S, Waldbieser G (2011) Mapping of the Toll-like receptor family in channel catfish, *Ictalurus punctatus*. Anim Genet 42:567–568

Quiniou SM, Boudinot P, Bengtén E (2013) Comprehensive survey and genomic characterization of Toll-like receptors (TLRs) in channel catfish, *Ictalurus punctatus*: identification of novel fish TLRs. Immunogenetics 65:511–530

Rebl A, Goldammer T, Seyfert H-M (2010) Toll-like receptor signaling in bony fish. Vet Immunol Immunopathol 134:139–150

Roach JC, Glusman G, Rowen L, Kaur A, Purcell MK, Smith KD, Hood LE, Aderem A (2005) The evolution of vertebrate Toll-like receptors. Proc Natl Acad Sci U S A 102:9577–9582

Rombout J, Koumans-van Diepen J, Emmer P, Taverne-Thiele J, Taverne N (1996) Characterization of carp thrombocytes with specific monoclonal antibodies. J Fish Biol 49:521–531

Ruszczyk A, Forlenza M, Joerink M, Ribeiro C, Jurecka P, Wiegertjes GF (2008) *Trypanoplasma borreli* cysteine proteinase activities support

a conservation of function with respect to digestion of host proteins in common carp. Dev Comp Immunol 32:1348–1361

Saitou N, Nei M (1987) The neighbor-joining method: a new method for reconstructing phylogenetic trees. Mol Biol Evol 4:406–425

Šali A, Blundell TL (1993) Comparative protein modelling by satisfaction of spatial restraints. J Mol Biol 234:779–815

Secombes C, Van Groningen J, Egberts E (1983) Separation of lymphocyte subpopulations in carp *Cyprinus carpio* L. by monoclonal antibodies: immunohistochemical studies. Immunology 48:165

Stolte EH, Savelkoul HF, Wiegertjes G, Flik G, Lidy Verburg-van Kemenade B (2008) Differential expression of two interferon-γ genes in common carp (*Cyprinus carpio* L.). Dev Comp Immunol 32:1467–1481

Sundaram AY, Kiron V, Dopazo J, Fernandes JM (2012) Diversification of the expanded teleost-specific toll-like receptor family in Atlantic cod, *Gadus morhua*. BMC Evol Biol 12:256

Tamura K, Peterson D, Peterson N, Stecher G, Nei M, Kumar S (2011) MEGA5: molecular evolutionary genetics analysis using maximum likelihood, evolutionary distance, and maximum parsimony methods. Mol Biol Evol 28:2731–2739

Veneman WJ, Stockhammer OW, de Boer L, Zaat SA, Meijer AH, Spaink HP (2013) A zebrafish high throughput screening system used for *Staphylococcus epidermidis* infection marker discovery. BMC Genomics 14:255

Yarovinsky F, Zhang D, Andersen JF, Bannenberg GL, Serhan CN, Hayden MS, Hieny S, Sutterwala FS, Flavell RA, Ghosh S (2005) TLR11 activation of dendritic cells by a protozoan profilin-like protein. Science 308:1626–1629

Yilmaz A, Shen S, Adelson DL, Xavier S, Zhu JJ (2005) Identification and sequence analysis of chicken Toll-like receptors. Immunogenetics 56:743–753

Zuckerkandl E, Pauling L (1965) Molecules as documents of evolutionary history. J Theor Biol 8:357–366